



Cite this: *Chem. Sci.*, 2022, **13**, 10048

All publication charges for this article have been paid for by the Royal Society of Chemistry

Subcomponent self-assembly of circular helical $Dy_6(L)_6$ and bipyramidal $Dy_{12}(L)_8$ architectures directed via second-order template effects[†]

Xiao-Lei Li, ^{ab} Lang Zhao, ^a Jianfeng Wu, ^a Wei Shi, ^{*b} Niklas Struch, ^c Arne Lützen, ^{*c} Annie K. Powell, ^{*de} Peng Cheng ^b and Jinkui Tang ^{*af}

In situ metal-templated (hydrazone) condensation also called subcomponent self-assembly of 4,6-dihydratino-pyrimidine, *o*-vanillin and dysprosium ions resulted in the formation of discrete hexa- or dodecanuclear metallosupramolecular $Dy_6(L)_6$ or $Dy_{12}(L)_8$ aggregates resulting from second-order template effects of the base and the lanthanide counterions used in these processes. XRD analysis revealed unique circular helical or tetragonal bipyramidal architectures in which the bis(hydrazone) ligand L adopts different conformations and shows remarkable differences in its mode of metal coordination. While a molecule of trimethylamine acts as a secondary template that fills the void of the $Dy_6(L)_6$ assembly, sodium ions take on this role for the formation of heterobimetallic $Dy_{12}(L)_8$ by occupying vacant coordination sites, thus demonstrating that these processes can be steered in different directions upon subtle changes of reaction conditions. Furthermore, $Dy_6(L)_6$ shows an interesting spin-relaxation energy barrier of 435 K, which is amongst the largest values within multinuclear lanthanide single-molecular magnets.

Received 3rd June 2022

Accepted 20th July 2022

DOI: 10.1039/d2sc03156f

rsc.li/chemical-science

Introduction

Oligonuclear metallosupramolecular complexes of lanthanides have attracted quite some interest over the last two decades mainly due to their astonishing photophysical and magnetic properties.¹ Nevertheless, their supramolecular chemistry is much less developed than that of d-block metals^{1a,b,2,3} as their coordination chemistry is more challenging to control – their generally large coordination numbers and geometries are much

less defined, and since their coordination chemistry is mainly governed by electrostatic interactions they neither show very distinct preferences for donor atoms such as nitrogen or oxygen; other than that, they should be rather hard Lewis-basic sites nor do classical supramolecular design principles such as the maximum site occupancy rule⁴ apply to them.^{1,5} Therefore, the use of ligand motifs that offer a high density of potential donor atoms has proven to be a successful approach to access metallosupramolecular aggregates of lanthanides *via* coordination-driven self-assembly processes although their outcome is still hard to predict.^{1,6}

The subcomponent self-assembly approach⁷ that involves reversible *in situ* metal-templated condensation reactions to form imine or hydrazone bonds has been established as a particularly powerful tool for generating metallosupramolecular architectures of increasing structural complexity with various properties and features,⁸ like for example, astonishing host–guest behavior,⁹ complex-to-complex transformations¹⁰ or switchable systems.^{10a,11} Moreover, subcomponent self-assembly also provides space for serendipity to form new structures, and thereby, discover new interesting general structural motifs and/or metal binding motifs which might not even necessarily make use of all subcomponents in the initially expected relative ratio. Thus, we regard it as an especially versatile approach to prepare oligonuclear metallosupramolecular aggregates with densely functionalized multi-functional metal binding motifs essential to address the specific needs of lanthanide coordination.

^aState Key Laboratory of Rare Earth Resource Utilization, Changchun Institute of Applied Chemistry, Chinese Academy of Sciences, Changchun 130022, P. R. China. E-mail: tang@ciac.ac.cn

^bKey Laboratory of Advanced Energy Materials Chemistry (Ministry of Education), College of Chemistry, Nankai University, Tianjin 300071, P. R. China. E-mail: shiwei@nankai.edu.cn

^cKekulé Institute of Organic Chemistry and Biochemistry, Rheinische-Friedrich-Wilhelms-University of Bonn, Gerhard-Domagk-Str. 1, D-53121 Bonn, Germany. E-mail: arne.luetzen@uni-bonn.de

^dInstitute of Inorganic Chemistry, Karlsruhe Institute of Technology, Engesserstrasse 15, 76131 Karlsruhe, Germany. E-mail: annie.powell@kit.edu

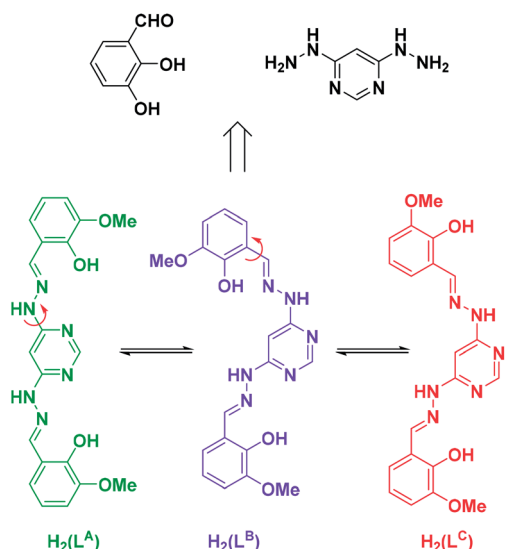
^eInstitute of Nanotechnology, Karlsruhe Institute of Technology, Hermann-von-Helmholtz-Platz 1, Eggenstein-Leopoldshafen, 76344 Karlsruhe, Germany

^fUniversity of Science and Technology of China, Hefei 230026, P. R. China

[†] Electronic supplementary information (ESI) available: Experimental details and additional figures (Tables S1–S8 and Fig. S1–S28. CCDC 1507720 and 1536333. For ESI and crystallographic data in CIF or other electronic format see <https://doi.org/10.1039/d2sc03156f>

[‡] Current address: Arlanxeo Deutschland GmbH, Alte Heerstraße 2, 41540 Dormagen, Germany.





Scheme 1 Ligand L derived from *o*-vanillin and 4,6-dihydrizinopyrimidine as its neutral form H₂(L) in three different conformations H₂(L^A), H₂(L^B) and H₂(L^C) relevant for this study. Red arrows indicate successive rotations around single bonds to convert the different conformers into each other. The different conformations give rise to different coordination modes as shown in Fig. 1 and 2.

Following our interest in the magnetic properties of oligonuclear lanthanide complexes,^{12,13} we decided to also apply this approach. Herein, we report on the use of *o*-vanillin and 4,6-dihydrizinopyrimidine as subcomponents that undergo twofold metal-templated hydrazone condensation and metal coordination upon mixing with lanthanide salts and a suitable base giving rise to rather surprising cyclic helical hexanuclear complexes or a dodecanuclear tetragonal bipyramidal complex as a result of secondary template effects. With this study we extend our previous work that demonstrated the validity of the flexible dianionic ligand L (Scheme 1), that results from the metal-templated twofold hydrazone formation of the organic subcomponents, in the construction of polynuclear lanthanide SMMs with desired topology and magnetic properties.¹⁴

Experimental

General synthetic considerations

All starting materials were of A.R. Grade and were used as commercially obtained without further purification. 4,6-Dihydrizinopyrimidine was prepared according to a previously published method.¹⁵ Elemental analyses for C, H, and N were carried out on a PerkinElmer 2400 analyzer. Fourier transform IR (FTIR) spectra were recorded with a PerkinElmer FTIR spectrophotometer using the reflectance technique (4000–300 cm^{–1}). The samples were prepared as KBr pellets. High-resolution mass spectra were acquired using a Thermo Scientific X series.

Synthesis of [Dy₆L^A₂L^C₄(CH₃OH)₇(H₂O)₅(NO₃)₄]

NET₃·10CH₃OH·11H₂O·2NO₃ (Dy₆L₆)

4,6-Dihydrizinopyrimidine (0.1 mmol) was dissolved in 15 mL methanol, and then *o*-vanillin (0.2 mmol) and NET₃ (0.2 mmol)

were added successively. Finally, Dy(NO₃)₃·6H₂O (0.1 mmol) was added to the mixture. The reaction mixture was stirred at room temperature for 4 h and the resultant solution was filtered and left unperturbed to allow for slow evaporation of the solvent. Dark yellow single crystals of complex Dy₆L₆ were obtained after one week. Yield: 25 mg, (31.95%, based on the metal salt). Elemental analysis (%) calcd for C₁₄₃Dy₆N₄₃O₇₅H₁₉₈: C, 36.59, H, 4.25, N, 12.83; found C, 36.52, H, 4.29, N, 12.78.

Synthesis of [Dy₁₂Na₄L^A₄L^B₄(CH₃COO)₁₂(C₈H₇O)₄(CO₃)₄(CH₃CN)₂(H₂O)₄]·6H₂O (Dy₁₂L₈)

4,6-Dihydrizinopyrimidine (0.1 mmol) was dissolved in methanol/acetonitrile (5 mL : 10 mL), and then *o*-vanillin (0.2 mmol) and NaHCO₃ (0.1 mmol) were added successively. Finally, Dy(OAc)₃·2H₂O (0.1 mmol) was added to the mixture. The reaction mixture was stirred at room temperature for 5 h and the resultant solution was filtered and left unperturbed to allow for slow evaporation of the solvent. Dark yellow single crystals of complex Dy₁₂L₈ were obtained after one week. Yield: 25 mg, (41.89%, based on the Dy^{III} salt). Elemental analysis (%) calcd for C₂₂₄H₂₂₂Dy₁₂N₅₀Na₄O₉₄: C, 20.46, H, 3.12, N, 9.78; found C, 20.39, H, 3.18, N, 9.84.

X-ray crystal structure determinations

Crystallographic data and refinement details are given in Table S2.[†] Single crystals of suitable dimensions of Dy₆(L)₆ and Dy₁₂(L)₈ were selected for single-crystal X-ray diffraction analysis. Crystallographic data were collected at 100(5) K on a Bruker Apex II CCD diffractometer with graphite monochromated Mo-K α radiation ($\lambda = 0.71073$ Å). The data were integrated using the Siemens SAINT program. Absorption corrections were applied. The structures were solved by direct methods and refined by the full-matrix least-squares method based on F^2 with anisotropic thermal parameters for all non-hydrogen atoms by using the SHELXS (direct methods) and refined by SHELXL (full matrix least-squares techniques) in the Olex2 package.¹⁶ The locations of Dy and Na atoms were easily determined, and O, N, and C atoms were subsequently determined from the different Fourier maps. Anisotropic thermal parameters were assigned to all non-hydrogen atoms. The H atoms were introduced in the calculated positions and refined with a fixed geometry with respect to their carrier atoms. CCDC 1507720 (Dy₆(L)₆) and 1536333 (Dy₁₂(L)₈) contain the supplementary crystallographic data for this paper.[†]

Magnetic measurements

Magnetic susceptibility measurements were recorded on a Quantum Design MPMS-XL7 SQUID magnetometer equipped with a 7 T magnet. The variable-temperature magnetizations were measured in the temperature range of 1.9–300 K with an external magnetic field of 1000 Oe. The dynamics of magnetization were investigated from the ac susceptibility measurements in the zero static fields and a 3.0 Oe ac oscillating field. Diamagnetic corrections were made with Pascal's constants¹⁷ for all the constituent atoms as well as the contributions of the sample holder.



Results and discussion

Structural analysis

Here, we dissolved 4,6-dihydrazinopyrimidine, *o*-vanillin and NET_3 (ref. 18) in methanol successively, and then added one equivalent of $\text{Dy}(\text{NO}_3)_3$ to the mixture.¹⁹ The initially light yellow solution slowly turned dark yellow and dark yellow crystals were obtained after one week. The crystals were macroscopically examined by optical microscopy and scanning electron microscopy (SEM), revealing their hexagonal shape (see the ESI†). ESI mass spectrometric investigations of the reaction mixtures as well as of the samples obtained upon dissolving the crystalline product revealed a $\text{Dy}_6(\text{L})_6$ stoichiometry of the resulting products (see the ESI†). This assumption could finally be proven by X-ray diffraction analysis of the single crystals of the hexanuclear dysprosium(III) complex. The result of the analysis is shown in Fig. 1 and it reveals the rather complicated and unique structure of the $\text{NET}_3 @ [\text{Dy}_6(\text{L})_6(\text{CH}_3\text{OH})_7(\text{H}_2\text{O})_5(\text{NO}_3)_4](\text{NO}_3)_2$ unit of this metallosupramolecular architecture. The six Dy^{III} ions adopt a distorted hexagonal arrangement with an average distance of 8.3 Å between them (the corresponding angles in this Dy_6 hexagon and the coordination geometries of the Dy^{III} ions are listed in the ESI†).

Each Dy^{III} center is coordinated by two metal binding motifs from two dianionic ligands L (Fig. 1d and the ESI†) and the remaining coordination sites are occupied by counter ions or solvent molecules. The ligands L , however, do not all have the same conformation, and therefore, do not bind in the same binding mode to all of the Dy^{III} centers. While two of these

ligands adopt conformation A (L^{A}) acting as a bis(tridentate) ligand bridging two adjacent metal centers in the periphery of the cyclic hexanuclear aggregate (see the green ligands in Fig. 1b), the other four adopt conformation C (L^{C}) which is why the structure could more precisely be described as a $[\text{Dy}_6(\text{L}^{\text{A}})_2(\text{L}^{\text{C}})_4(\text{CH}_3\text{OH})_7(\text{H}_2\text{O})_5(\text{NO}_3)_4]^{2+}$ unit (see the red ligands in Fig. 1b). As such, ligands L^{C} bridge the metal centers in a mixed tri- and bidentate binding mode in a grid like fashion leading to an overall helically interwoven architecture as illustrated in Fig. 1c (see the ESI† for other representations). Thus, two opposite Dy^{III} centers are coordinated by the tridentate binding sites of two ligands L^{C} whereas the other four are coordinated by one tridentate binding site of a ligand L^{A} and the bidentate binding motif of a ligand L^{C} .

It is noteworthy that many lanthanide-based double,⁵ triple,²⁰ and quadruple-stranded²¹ helicates assembled using flexible ligands have been reported, which generally display ordinary linear topology, while for lanthanide-based circular helicates, only very few examples have been reported to date, including triangular,²² square²³ and hexagonal^{21,24} diverse topologies.^{1g} Therefore, the circular helicate $\text{Dy}_6(\text{L})_6$ indeed belongs to the rather rare species considering that the bridging ligand L adopts different conformations (L^{A} and L^{C} , Fig. 1 and the ESI†).

Due to this arrangement, the aggregate contains a rather hydrophobic cavity which is occupied by a molecule of trimethylamine which perfectly fills this void. Such (secondary) template effects are rather common in the formation of cyclic or cage-like self-assembled structures whose components can also assemble into other spatial arrangements in the absence of

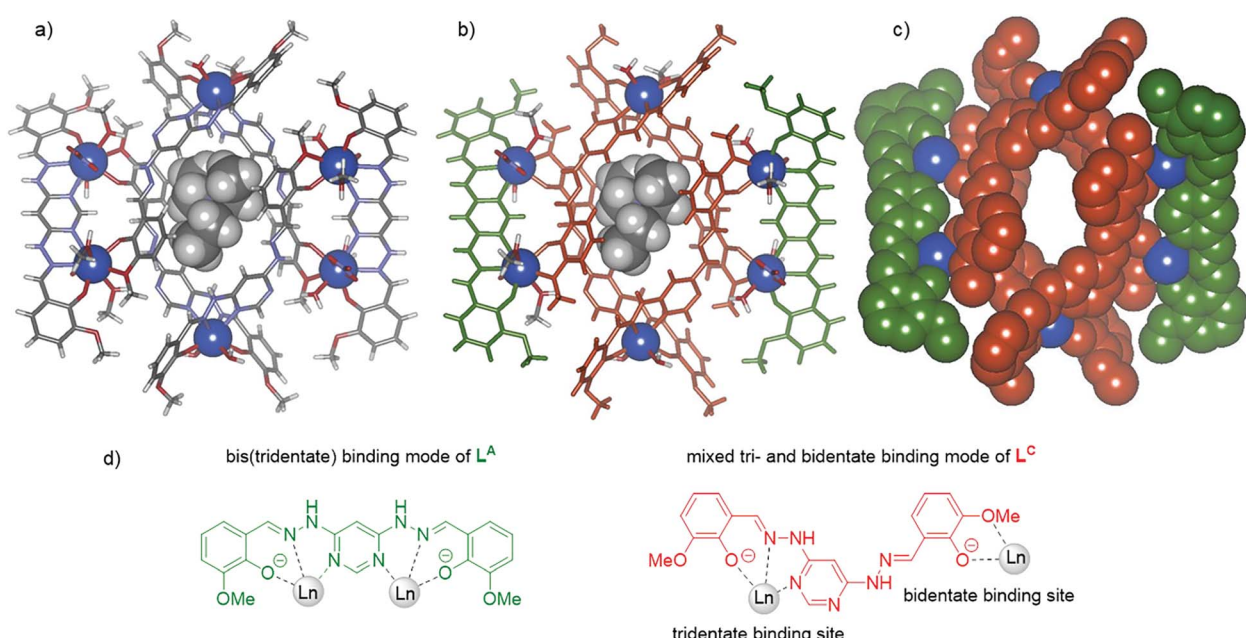


Fig. 1 (a) Structure of the cationic unit of $[\text{Dy}_6(\text{L}^{\text{A}})_2(\text{L}^{\text{C}})_4(\text{CH}_3\text{OH})_7(\text{H}_2\text{O})_5(\text{NO}_3)_4](\text{NO}_3)_2$ as determined by X-ray diffraction analysis: (a) wire-and-sphere representation of the supramolecular aggregate where the NET_3 molecule occupying the central cavity is shown as a space-filling model (color code: C gray, H white, N light blue, O red, and Dy dark blue); (b) the same representation where ligands L^{A} and L^{C} have been colored in green and red as in Scheme 1, respectively; (c) space filling representation (coordinating nitrate ions and water and methanol molecules as well as the encapsulated molecule of trimethylamine are omitted, colour code as in (b)); (d) representation of the different binding modes of ligands L^{A} and L^{C} in this assembly.



a fitting template.^{2g,8a-c,25} Hence, we assume that triethylamine and basic molecules of similar shape²⁶ act as secondary templates for the formation of this aesthetically appealing supramolecular aggregate.

In order to test this and the influence of the counter ion further, we also investigated a subcomponent self-assembly approach using Dy(OAc)_3 and NaHCO_3 (ref. 18) as the base. Again, we were able to obtain the product of this approach in the form of yellow circular bipyramidal-shaped single crystals (see the ESI†) already indicating that another metallosupramolecular aggregate has been formed. Fortunately, the quality of the crystals was good enough to perform an XRD analysis that revealed yet another unique complex hexadecanuclear heterobimetallic architecture ($[(\text{Dy}_{12}\text{Na}_4(\text{L})_8(\text{CH}_3\text{COO})_{12}(\text{C}_8\text{H}_7\text{O})_4(\text{CO}_3)_4(\text{CH}_3\text{CN})_2(\text{H}_2\text{O})_4]\cdot 6\text{H}_2\text{O}$) (Fig. 2). The asymmetric unit of the structure contains three Dy^{III} ions and one Na^+ ion with one of the Dy^{III} centers being eight-coordinated whereas the other two are nine-coordinated (see the ESI†). The whole aggregate can be divided into three parts: two identical $\text{Dy}_4(\text{L})_2$ units featuring a dense arrangement of four Dy^{III} centers that are bridged by carbonates, acetates and solvate molecules where the Dy^{III} centers also bind in pairs to two ligands in conformation B (L^{B} , shown in purple in Fig. 2b) in a mixed tri- and bidentate fashion, as depicted in Fig. 2c (the other coordination sites of the Dy^{III} ions of these units are occupied by acetates). The third unit is a grid-like $\text{Dy}_4(\text{L})_4$ unit where each Dy^{III} center coordinates to tridentate binding sites of two ligands in

conformation A (L^{A} , shown in green in Fig. 2b). Interestingly, not all organic subcomponents assemble to ligand L here but the remaining coordination sites of each Dy^{III} ion are occupied by one molecule of *o*-vanillin (light blue in Fig. 2b) and a water molecule. These three units are held together by four sodium ions that coordinate as secondary templates to the remaining binding sites of the ligands L^{A} and L^{B} each in a chelating manner, as depicted in Fig. 2c. This results in an overall tetragonal bipyramidal $[(\text{Dy}_{12}\text{Na}_4(\text{L}^{\text{A}})_4(\text{L}^{\text{B}})_4(\text{CH}_3\text{COO})_{12}(\text{C}_8\text{H}_7\text{O})_4(\text{CO}_3)_4(\text{CH}_3\text{CN})_2(\text{H}_2\text{O})_4]\cdot 6\text{H}_2\text{O}$ architecture in which the two $\text{Dy}_4(\text{L}^{\text{B}})_2$ units form a $\text{Na}_4\text{Dy}_8(\text{L}^{\text{B}})_4$ cage that embeds the grid-like $\text{Dy}_4(\text{L}^{\text{A}})_4$ unit in its center (for additional representations of this unique assembly see the ESI†).

Both discrete metallosupramolecular aggregates belong to the rather rare species in which a bridging ligand adopts more than one conformation.^{25h,27} However, in these two new examples the ligands also differ significantly in their coordination behavior with regard to the binding sites for the metal ions and their denticity. This is special and a feature of metallosupramolecular assemblies of lanthanide ions because they tend to fill vacant coordination sites with counter ions and solvate molecules as capping or bridging ligands much more easily than transition metal ions due to the by far predominant electrostatic nature of the lanthanides' coordinative interactions with their ligands. That way, both assemblies achieve a favorable filling of space as well as a mutual orientation of

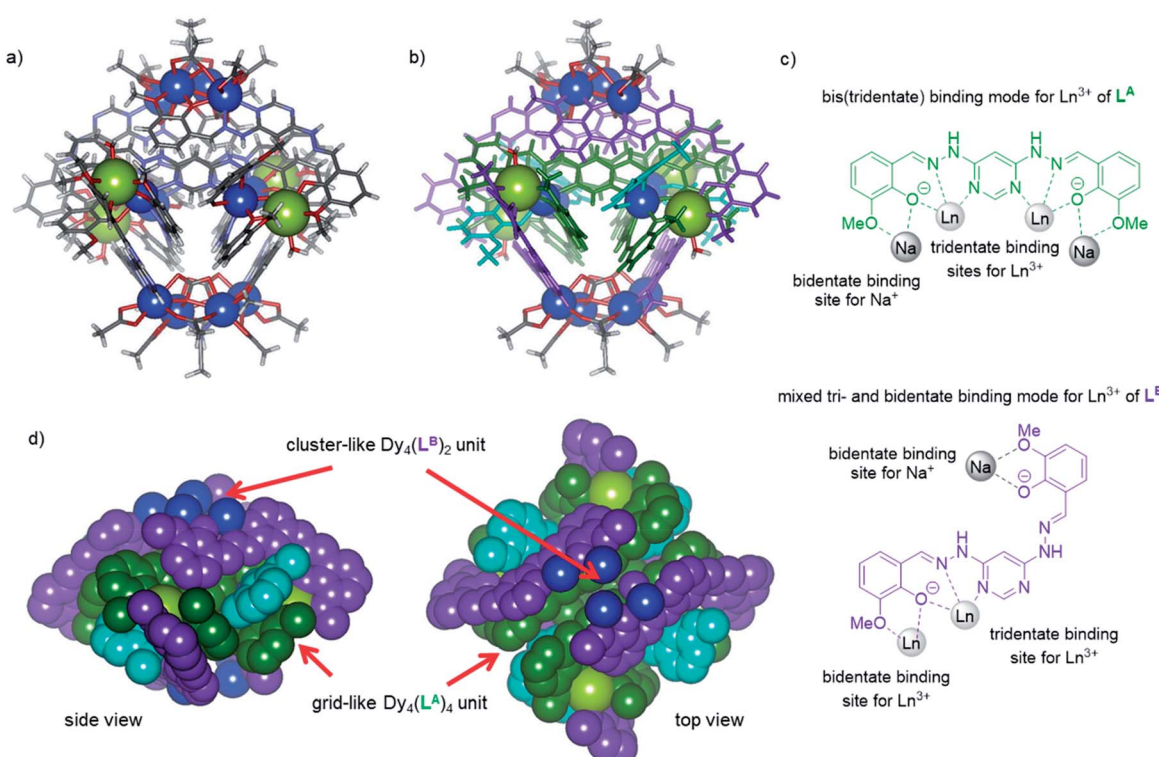


Fig. 2 (a-d) Structure of the $[(\text{Dy}_{12}\text{Na}_4(\text{L}^{\text{A}})_4(\text{L}^{\text{B}})_4(\text{CH}_3\text{COO})_{12}(\text{C}_8\text{H}_7\text{O})_4(\text{CO}_3)_4(\text{CH}_3\text{CN})_2(\text{H}_2\text{O})_4]\cdot 6\text{H}_2\text{O}$ unit as determined by X-ray diffraction analysis: (a) wire-and-sphere representation of the supramolecular aggregate (color code: C gray, H white, N light blue, O red, Dy dark blue, and Na yellow-green); (b) the same representation where ligands L^{A} and L^{B} and the *o*-vanillin molecules have been colored in green, purple and light blue, respectively; (c) representation of the different binding modes of ligands L^{A} and L^{B} in this assembly; (d) space filling representation from two perspectives (coordinating acetate and carbonate ions and acetonitrile and water are omitted, colour code as in (b)).



ligands L^A and L^B to ensure $\pi-\pi$ -interactions in $Dy_{12}(L)_8$ which most likely provide the driving forces for their formation.

Magnetic properties

Having elucidated the unexpected new structural motifs of the hexa- and dodecanuclear metallosupramolecular $Dy_6(L)_6$ and $Dy_{12}(L)_8$ assemblies, we wanted to see how this reflects in the complex properties. Therefore, we turned to explore their magnetic behavior and their ability to act as a lanthanide single-molecule magnet.^{1c,e,g,k,m,n,28} The variable-temperature χ_{MT} products (Fig. 3 and the ESI†) for $Dy_6(L)_6$ and $Dy_{12}(L)_8$ show similar trends with room-temperature χ_{MT} values of 83.98 and 168.98 $\text{cm}^3 \text{K mol}^{-1}$ corresponding to the expected values for uncoupled Dy^{III}_6 and Dy^{III}_{12} moieties ($^6H_{15/2}$, $S = 5/2$, $L = 5$, $J = 15/2$, $g = 4/3$). Upon lowering the temperature, the χ_{MT} values are weakly temperature dependent in both cases until below 70 K where they start to gradually fall, reaching values of 77.90 and 154.88 $\text{cm}^3 \text{K mol}^{-1}$ at 50 K, after which they precipitously decrease to reach 68.17 and 130.75 $\text{cm}^3 \text{K mol}^{-1}$ at 2.0 K.

The decrease observed in the χ_{MT} values suggests the magnetic anisotropy/ligand field and thermal depopulation of the excited M_J states, but we cannot preclude the presence of weak antiferromagnetic interactions in view of these poly-nuclear systems. Furthermore, the field dependence of the magnetization measurements shows a rapid increase at low fields and eventually reaches values of about $29.31 \mu_B$ for $Dy_6(L)_6$ and $62.83 \mu_B$ for $Dy_{12}(L)_8$ without clear saturation up to

70 kOe below 1.9 K, respectively (Fig. 3 and the ESI†). Additionally, in contrast to the non-superposition of the M vs. H/T data on to a single master-curve for $Dy_{12}(L)_8$, the nearly overlapping M versus H/T curves at different temperatures (see the ESI†) imply that there are well separated high excited-energy levels for $Dy_6(L)_6$ (see the ESI†). In addition, a butterfly-shaped magnetic hysteresis loop can be detected at 1.9 K, indicative of the presence of fast quantum tunnelling of the magnetization process in $Dy_6(L)_6$.

To verify SMM behavior, the frequency- and temperature-dependent AC susceptibilities of $Dy_6(L)_6$ and $Dy_{12}(L)_8$ were measured in a zero DC field (see the ESI†). For $Dy_{12}(L)_8$, no obvious χ'' signal was observed in the temperature-dependent AC measurements, suggesting the presence of fast quantum tunneling relaxation of magnetization. By contrast, significant slow relaxation of magnetization is observed in the AC susceptibility measurements for $Dy_6(L)_6$ (Fig. 3). The well-defined frequency-dependent maxima up to 35 K and strong frequency dependence of the AC susceptibilities both demonstrate SMM behavior with a large thermal energy barrier (see the ESI†). Two closely spaced relaxation processes operate in the high-temperature regime as seen from the broad χ'' peak and significantly broadened Cole–Cole plots (see the ESI†). The observation of two relaxation processes is common in multi-nuclear lanthanide systems and results from the two groups of distinct anisotropic centers in $Dy_6(L)_6$ (see the ESI†).²⁹

The relaxation times (τ) for these two processes can be extracted from the excellent fit of the sum of two modified Debye functions (see the ESI†). The fitting of the data is in good agreement with the data for $Dy_6(L)_6$ over the entire temperature range with effective energy barriers of $U_{\text{eff}1} = 435 \text{ K}$ (pre-exponential factor $\tau_{01} = 8.98 \times 10^{-10} \text{ s}$) and $U_{\text{eff}2} = 254 \text{ K}$ ($\tau_{02} = 7.4 \times 10^{-9} \text{ s}$) for the slow relaxation (SR) and fast relaxation (FR) phases, respectively (see the ESI†). We also obtain parameters of $C_1 = 2.0295 \times 10^{-5} \text{ s}^{-1} \text{K}^{-5.3}$, $n_1 = 5.3$ and $C_2 = 3.4718 \times 10^{-4} \text{ s}^{-1} \text{K}^{-5.09}$, and $n_2 = 5.09$ for SR and FR processes, respectively (Fig. 4).

In addition, the α values extracted from the sum of two modified Debye functions are less than 0.16 for SR, (see the

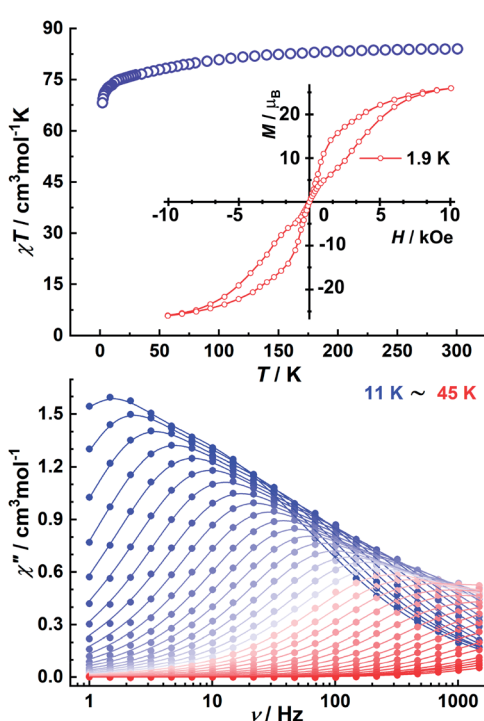


Fig. 3 χT vs. T plot recorded on $Dy_6(L)_6$ in an applied field of 1 kOe. Inset: molar magnetization at 1.9 K (top) and frequency dependence of the χ'' of $Dy_6(L)_6$ between 11 and 45 K (bottom). The solid lines represent the fitting of the experimental data using the sum of two modified Debye functions.

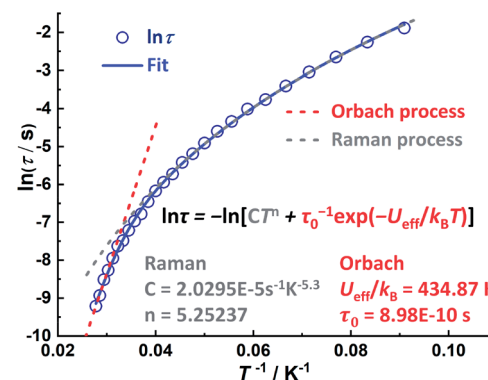


Fig. 4 A plot of $\ln(\tau/s)$ versus T^{-1} for SR of $Dy_6(L)_6$ under a zero dc-field; the relaxation times were obtained by simultaneous fitting of the Cole–Cole plots (Fig. S25†). The blue line represents the fit to multiple relaxation processes using eqn (S1).† Red and grey dashed lines represent individual Orbach and Raman fits, respectively.



ESI[†]) suggesting a relatively narrow distribution of the relaxation times. In contrast, the large α values (as large as 0.38) for FR indicate a wide distribution of relaxation times. Thus, $\text{Dy}_6(\text{L})_6$ represents an interesting example of an oligonuclear Dy^{III} SMM due to its unique closed helical structure and its effective energy barrier for the spin relaxation process of 435 K which is amongst the largest values within multinuclear lanthanide SMMs (see the ESI[†]).³⁰

Conclusion

In conclusion, we have shown how subcomponent self-assembly can give rise to facile ligand synthesis and spontaneous formation of two very different hexa- and dodecanuclear lanthanide metallosupramolecular architectures by employing the different second-order template effects arising from the base and the dysprosium's counterions. While the base trimethylamine acts as an efficient secondary template to favor the formation of a hexanuclear $\text{Dy}_6(\text{L})_6$ assembly by perfect space filling of the assembly's central void, the sodium ions from sodium bicarbonate act as secondary templates by being capable of occupying vacant coordination sites, and hence, lead to the formation of the $\text{Dy}_{12}(\text{L})_8$ aggregate. This highlights the possibilities for *in situ* formation of flexible ligand structures furnished with multiple donor centers that offer a plethora of different bi- or tridentate metal binding sites that can adopt different conformations to access different complicated metallosupramolecular architectures by rather subtle changes in the subcomponent self-assembly process.

$\text{Dy}_6(\text{L})_6$ not only has an extraordinary structure but it also exhibits clear butterfly-shaped magnetic hysteresis at 1.9 K and one of the largest energy barriers of 435 K within multinuclear lanthanide SMMs.

Thus, we envision this strategy to be very promising to address the formation of new (supra-)molecular structures with complex topologies and to learn more about how to understand, and ultimately predict, the self-assembly of lanthanide-based systems in a similarly reliable way as is already possible for transition metal systems.

Data availability

All data used to reach the results presented in this manuscript can be found in the ESI.[†]

Author contributions

J. T. conceived and designed the project. X.-L. L. carried out the synthesis and characterization studies, with the help of L. Z., J. W., W. S. and P. C. J. T. planned and executed the magnetic measurements and analysed the data. N. S. and A. L. analysed the ESI mass spectra. X.-L. L., J. T., A. L. and A. K. P. wrote the manuscript, with contributions from all the co-authors.

Conflicts of interest

The authors declare no conflict of interest.

Acknowledgements

We thank the National Natural Science Foundation of China (21871247, 21801237 and 21971123), the Key Research Program of Frontier Sciences, CAS (ZDBS-LY-SLH023), the Key Research Program of the Chinese Academy of Sciences (ZDRW-CN-2021-3-3), the National Science and Technology Major Project (2020YFE0204500), the Natural Science Foundation of Jilin Province of China (20200201244JC), the China Postdoctoral Science Foundation (2021M693397) and the POF STN of the Helmholtz Foundation for financial support. X.-L. L. is thankful to the Chinese Academy of Sciences for a Special Research Assistant Grant (2021000162). J. T. gratefully acknowledges support of the Royal Society-Newton Advanced Fellowship (NA160075). N. S. is thankful to the Evonik Foundation for a doctoral grant.

References

- (a) M. Albrecht, *Chem. Rev.*, 2001, **101**, 3457; (b) J.-C. G. Bünzli and C. Piguet, *Chem. Rev.*, 2002, **102**, 1897; (c) G. Benelli and D. Gateschi, *Chem. Rev.*, 2002, **102**, 2369; (d) J.-C. G. Bünzli and C. Piguet, *Chem. Soc. Rev.*, 2005, **34**, 1048; (e) R. Sessoli and A. K. Powell, *Coord. Chem. Rev.*, 2009, **253**, 2328; (f) S. V. Eliseeva and J.-C. G. Bünzli, *Chem. Soc. Rev.*, 2010, **39**, 189; (g) S. V. Eliseeva and J.-C. G. Bünzli, *New J. Chem.*, 2011, **35**, 1165; (h) P. Zhang, Y.-N. Guo and J. Tang, *Coord. Chem. Rev.*, 2013, **257**, 1728; (i) S. J. Bradberry, A. J. Savyasachi, M. Martinez-Calvo and T. Gunnlaugsson, *Coord. Chem. Rev.*, 2014, **273–274**, 226; (j) J.-C. G. Bünzli, *J. Coord. Chem.*, 2014, **67**, 3706; (k) K. Liu, X. Zhang, X. Meng, W. Shi, P. Cheng and A. K. Powell, *Chem. Soc. Rev.*, 2016, **45**, 2423; (l) D. E. Barry, D. F. Caffrey and T. Gunnlaugsson, *Chem. Soc. Rev.*, 2016, **45**, 3244; (m) Z. Zhu, M. Guo, X.-L. Li and J. Tang, *Coord. Chem. Rev.*, 2019, **378**, 350; (n) X.-L. Li and J. Tang, *Dalton Trans.*, 2019, **48**, 15358; (o) X. Liu and J.-R. Hamon, *Coord. Chem. Rev.*, 2019, **389**, 94; (p) H.-Y. Wong, W.-S. Lo, K.-H. Yim and G.-L. Law, *Chem.*, 2019, **5**, 3058; (q) X.-Z. Li, C.-B. Tian and Q.-F. Sun, *Chem. Rev.*, 2022, **122**, 6374.
- For some reviews on structural aspects see: (a) K. Suzuki, M. Tominaga, M. Kawano and M. Fujita, *Chem. Commun.*, 2009, **45**, 1638; (b) R. Chakrabaty, P. S. Mukherjee and P. J. Stang, *Chem. Rev.*, 2011, **111**, 5810; (c) T. R. Cook, Y. R. Zheng and P. J. Stang, *Chem. Rev.*, 2013, **113**, 734; (d) M. M. J. Smulders, I. A. Riddell, C. Browne and J. R. Nitschke, *Chem. Soc. Rev.*, 2013, **42**, 1728; (e) K. Harris, D. Fujita and M. Fujita, *Chem. Commun.*, 2013, **49**, 6703; (f) S. Mukherjee and P. S. Mukherjee, *Chem. Commun.*, 2014, **50**, 2239; (g) M. Han, D. M. Engelhard and G. H. Clever, *Chem. Soc. Rev.*, 2014, **43**, 1848; (h) L. Chen, Q. Chen, M. Wu, F. Jiang and M. Hong, *Acc. Chem. Res.*, 2015, **48**, 201; (i) H. Li, Z.-J. Yao, D. Liu and G.-X. Jin, *Coord. Chem. Rev.*, 2015, **293–294**, 139; (j) T. R. Cook and P. J. Stang, *Chem. Rev.*, 2015, **115**, 7001; (k) L.-J. Chen, H.-B. Yang and M. Shinoya, *Chem. Soc. Rev.*, 2017, **46**, 2555; (l) Y.-Y. Zhang, W.-X. Gao, L. Lin and G.-X. Jin, *Coord. Chem. Rev.*, 2017,



344, 323; (m) Q. Yang and J. Tang, *Dalton Trans.*, 2019, **48**, 769.

3 For some reviews on functional aspects see: (a) D. Fielder, D. H. Leung, R. G. Bergman and K. N. Raymond, *Acc. Chem. Res.*, 2005, **38**, 349; (b) M. Fujita, M. Tominaga, A. Hori and B. Therrien, *Acc. Chem. Res.*, 2005, **38**, 369; (c) M. J. Hannon, *Chem. Soc. Rev.*, 2007, **36**, 280; (d) H. Amouri, C. Desmarests, A. Bettoschi, M. N. Rager, K. Boubekeur, P. Rabu and M. Drillon, *Chem.-Eur. J.*, 2007, **13**, 5401; (e) A. Bousseksou, G. Molnár, J. A. Real and K. Tanaka, *Coord. Chem. Rev.*, 2007, **251**, 1822; (f) J. A. Kitchen and S. Brooker, *Coord. Chem. Rev.*, 2008, **252**, 2072; (g) M. Yoshizawa, J. K. Klosterman and M. Fujita, *Angew. Chem., Int. Ed.*, 2009, **48**, 3418; (h) J. Olgún and S. Brooker, *Coord. Chem. Rev.*, 2011, **255**, 203; (i) T. R. Cook, V. Vajpayee, M. H. Lee, P. J. Stang and K.-W. Chi, *Acc. Chem. Res.*, 2013, **46**, 2464; (j) M. D. Ward and P. R. Raithby, *Chem. Soc. Rev.*, 2013, **42**, 1619; (k) M. L. Saha, S. Neogi and M. Schmittel, *Dalton Trans.*, 2014, **43**, 3815; (l) X. Yan, T. R. Cook, P. Wang, F. Huang and P. J. Stang, *Nat. Chem.*, 2015, **7**, 342; (m) S. Zarra, D. M. Wood, D. A. Roberts and J. R. Nitschke, *Chem. Soc. Rev.*, 2015, **44**, 419; (n) S. H. A. M. Leenders, R. Gramaglia-Doria, B. de Bruin and J. N. H. Reek, *Chem. Soc. Rev.*, 2015, **44**, 433; (o) C. J. Brown, F. D. Toste, R. G. Bergman and K. N. Raymond, *Chem. Rev.*, 2015, **115**, 3012; (p) J. E. M. Lewis, P. D. Beer, S. J. Loeb and S. M. Goldup, *Chem. Soc. Rev.*, 2017, **46**, 2577; (q) R. W. Hogue, S. Singh and S. Brooker, *Chem. Soc. Rev.*, 2018, **47**, 7303; (r) M. Hardy and A. Lützen, *Chem.-Eur. J.*, 2020, **26**, 13332.

4 (a) R. Krämer, J.-M. Lehn and A. Marquis-Rigault, *Proc. Natl. Acad. Sci. U. S. A.*, 1993, **90**, 5394; (b) S. De, K. Mahata and M. Schmittel, *Chem. Soc. Rev.*, 2010, **39**, 1555.

5 J.-F. Lemomnnier, L. Guénée, G. Bernardinelli, J. F. Vigier, B. Bocquet and C. Piguet, *Inorg. Chem.*, 2010, **49**, 1252.

6 A. Adhikary, H. S. Jena, S. Khatua and S. Konar, *Chem.-Asian J.*, 2014, **9**, 1083.

7 A. M. Castilla, W. J. Ramsay and J. R. Nitschke, *Acc. Chem. Res.*, 2014, **47**, 2063.

8 (a) J.-F. Ayme, J. E. Beves, D. A. Leigh, R. T. McBurney, K. Rissanen and D. Schultz, *Nat. Chem.*, 2012, **4**, 15; (b) J.-F. Ayme, J. E. Beves, D. A. Leigh, R. T. McBurney, K. Rissanen and D. Schultz, *J. Am. Chem. Soc.*, 2012, **134**, 9488; (c) J.-F. Ayme, J. E. Beves, C. J. Campbell and D. A. Leigh, *Angew. Chem., Int. Ed.*, 2014, **53**, 7823; (d) X.-P. Zhou, Y. Wu and D. Li, *J. Am. Chem. Soc.*, 2013, **135**, 16062; (e) S. Hong, M. R. Rohman, J. Jia, Y. Kim, D. Moon, Y. Kim, Y. H. Ko, E. Lee and K. Kim, *Angew. Chem., Int. Ed.*, 2015, **54**, 13241; (f) P. D. Frischmann, V. Kunz, V. Stepaneko and F. Würthner, *Chem.-Eur. J.*, 2015, **21**, 2766–2769; (g) P. D. Frischmann, V. Kunz and F. Würthner, *Angew. Chem., Int. Ed.*, 2015, **54**, 7285; (h) C. J. E. Haynes, J. Zhu, C. Chimerel, S. Hernández-Ainsa, I. A. Riddell, T. K. Ronson, U. F. Keyser and J. R. Nitschke, *Angew. Chem., Int. Ed.*, 2017, **56**, 15388; (i) R. Saha, D. Samanta, A. J. Bhattacharyya and P. S. Mukherjee, *Chem.-Eur. J.*, 2017, **23**, 8980; (j) M. Hardy, N. Struch, F. Topić, G. Schnakenburg, K. L. Rissanen and A. Lützen, *Inorg. Chem.*, 2018, **57**, 3507; (k) I. Sinha and P. S. Mukherjee, *Inorg. Chem.*, 2018, **57**, 4205; (l) D. Zhang, T. K. Ronson, J. Mosquera, A. Martinez and J. R. Nitschke, *Angew. Chem., Int. Ed.*, 2018, **57**, 3717; (m) J. Anhäuser, R. Puttreddy, L. Glanz, A. Schneider, M. Engeser, K. Rissanen and A. Lützen, *Chem.-Eur. J.*, 2019, **25**, 12294.

9 (a) M. C. Young, L. R. Holloway, A. M. Johnson and R. J. Hooley, *Angew. Chem., Int. Ed.*, 2014, **53**, 9832; (b) W. J. Ramsay, F. J. Rizzuto, T. K. Ronson, K. Caprice and J. R. Nitschke, *J. Am. Chem. Soc.*, 2016, **138**, 7264; (c) T. K. Ronson, B. S. Pilgrim and J. R. Nitschke, *J. Am. Chem. Soc.*, 2016, **138**, 10417; (d) S.-J. Hu, X.-Q. Guo, L.-P. Zhou, D.-N. Yan, P.-M. Cheng, L.-X. Cai, X.-Z. Li and Q.-F. Sun, *J. Am. Chem. Soc.*, 2022, **144**, 4244.

10 (a) P. Mal, D. Schultz, K. Beyeh, K. Rissanen and J. R. Nitschke, *Angew. Chem., Int. Ed.*, 2008, **47**, 8297; (b) W. Meng, T. K. Ronson, J. K. Clegg and J. R. Nitschke, *Angew. Chem., Int. Ed.*, 2013, **52**, 1017; (c) X.-P. Zhou, Y. Wu and D. Li, *J. Am. Chem. Soc.*, 2013, **135**, 16062; (d) D. Samanta and P. S. Mukherjee, *Chem.-Eur. J.*, 2014, **20**, 12483; (e) A. J. McConnell, C. M. Aitchison, A. B. Grommet and J. R. Nitschke, *J. Am. Chem. Soc.*, 2017, **139**, 6294; (f) N. Struch, F. Topić, K. Rissanen and A. Lützen, *Dalton Trans.*, 2017, **46**, 10809; (g) N. Struch, F. Topić, G. Schnakenburg, K. Rissanen and A. Lützen, *Inorg. Chem.*, 2018, **57**, 241; (h) M. Hardy, N. Struch, J. J. Holstein, G. Schnakenburg, N. Wagner, M. Engeser, J. Beck, G. H. Clever and A. Lützen, *Angew. Chem., Int. Ed.*, 2020, **59**, 3195.

11 (a) D.-H. Ren, D. Qiu, C.-Y. Pang, Z. Li and Z.-G. Gu, *Chem. Commun.*, 2015, **51**, 788–791; (b) N. Struch, G. Schnakenburg, R. Weisbarth, S. Klos, J. Beck and A. Lützen, *Dalton Trans.*, 2016, **45**, 14023–14029; (c) N. Struch, C. Bannwarth, T. K. Ronson, Y. Lorenz, B. Mienert, N. Wagner, M. Engeser, E. Bill, R. Puttreddy, K. Rissanen, J. Beck, S. Grimme, J. R. Nitschke and A. Lützen, *Angew. Chem., Int. Ed.*, 2017, **56**, 4930; (d) A. J. McConnell, *Supramol. Chem.*, 2018, **30**, 858; (e) M. Hardy, J. Tessarolo, J. J. Holstein, N. Struch, N. Wagner, R. Weisbarth, M. Engeser, J. Beck, S. Horiuchi, G. H. Clever and A. Lützen, *Angew. Chem., Int. Ed.*, 2021, **60**, 22562.

12 For some recent examples see: (a) S.-Y. Lin, W. Wernsdorfer, L. Ungur, A. K. Powell, Y.-N. Guo, J. Tang, L. Zhao, L. F. Chibotaru and H.-J. Zhang, *Angew. Chem., Int. Ed.*, 2016, **55**, 15574; (b) X. Zhang, S. Liu, V. Vieru, N. Xu, C. Gao, B.-W. Wang, W. Shi, L. F. Chibotaru, S. Gao, P. Cheng and A. K. Powell, *Chem.-Eur. J.*, 2018, **24**, 6079; (c) V. Vieru, L. Ungur, V. Cemortan, A. Sukhanov, A. Baniodeh, C. E. Anson, A. K. Powell, V. Voronkova and L. F. Chibotaru, *Chem.-Eur. J.*, 2018, **24**, 16652; (d) L. Chertan, S. F. M. Schmidt, H. Aueerbach, T. Hochdörffer, J. A. Wollny, W. Bi, J. Zhao, M. Y. Hu, T. Toellner, E. E. Alp, D. E. Brown, C. E. Anson, A. K. Powell and V. Schünemann, *Angew. Chem., Int. Ed.*, 2019, **58**, 3444; (e) K. Griffiths, I. A. Kuhne, G. J. Tizzard,



S. J. Coles, G. E. Kostakis and A. K. Powell, *Inorg. Chem.*, 2019, **58**, 2483; (f) T. Bereta, A. Mondal, K. Slepokura, Y. Peng, A. K. Powell and J. Lisowski, *Inorg. Chem.*, 2019, **58**, 4201; (g) Y. Peng, M. K. Singh, V. Mereacre, C. E. Anson, G. Rajamaran and A. K. Powell, *Chem. Sci.*, 2019, **10**, 5528; (h) M. Perfetti, J. Rinck, G. Cucinotta, C. E. Anson, Y. Gong, L. Ungur, L. Chibotura, M.-E. Boulon, A. K. Powell and R. Sessoli, *Front. Chem.*, 2019, **7**, 6; (i) A. Khan, O. Fuhr, M. N. Akhtar, Y. Lan, M. Thomas and A. K. Powell, *J. Coord. Chem.*, 2020, **73**, 1045; (j) P. Hahn, S. Ullmann, J. Klose, Y. Peng, A. K. Powell and B. Kersting, *Dalton Trans.*, 2020, **49**, 10901; (k) H. Kaemmerer, A. Baniodeh, Y. Peng, E. Moreno-Pineda, M. Schulze, C. E. Anson, W. Wernsdorfer, J. Schnack and A. K. Powell, *J. Am. Chem. Soc.*, 2020, **142**, 14838.

13 For some recent examples see: (a) J. Wu, J. Jung, P. Zhang, H. Zhang, J. Tang and B. Le Guennic, *Chem. Sci.*, 2016, **7**, 3632; (b) X.-L. Li, J. Wu, L. Zhao, W. Shi, P. Cheng and J. Tang, *Chem. Commun.*, 2017, **53**, 3026; (c) J. Wu, M. Guo, X.-L. Li, L. Zhao, Q.-F. Sun, R. A. Layfield and J. Tang, *Chem. Commun.*, 2018, **54**, 12097; (d) Y. Zhang, B. Ali, J. Wu, M. Guo, Y. Yu, Z. Liu and J. Tang, *Inorg. Chem.*, 2019, **58**, 3167; (e) J. Lu, X.-L. Li, Z. Zhu, S. Liu, Q. Yang and J. Tang, *Dalton Trans.*, 2019, **48**, 14062; (f) J. Lu, X.-L. Li, C. Jin, Y. Yu and J. Tang, *New J. Chem.*, 2020, **44**, 994; (g) C. Jin, X.-L. Li, Z. Liu, A. Mansikkamäki and J. Tang, *Dalton Trans.*, 2020, **49**, 10477; (h) Z. Zhu, Y.-Q. Zhang, X.-L. Li, M. Guo, J. Lu, S. Liu, A. Layfield Richard and J. Tang, *CCS Chem.*, 2021, **3**, 388; (i) Z. Zhu, C. Zhao, T. Feng, X. Liu, X. Ying, X.-L. Li, Y.-Q. Zhang and J. Tang, *J. Am. Chem. Soc.*, 2021, **143**, 10077; (j) Z. Zhu, C. Zhao, Q. Zhou, S. Liu, X.-L. Li, A. Mansikkamäki and J. Tang, *CCS Chem.*, 2022, DOI: [10.31635/ceschem.022.202101604](https://doi.org/10.31635/ceschem.022.202101604).

14 X. L. Li, H. Li, D. M. Chen, C. Wang, J. Wu, J. Tang, W. Shi and P. Cheng, *Dalton Trans.*, 2015, **44**, 20316.

15 M. B. Bushuev, V. P. Krivopalov, N. V. Semikolenova, Y. G. Shvedenkov, L. A. Sheludyakova, G. G. Moskalenko, L. G. Lavrenova, V. A. Zakharov and S. V. Larionov, *Russ. J. Coord. Chem.*, 2007, **33**, 601.

16 O. V. Dolomanov, L. J. Bourhis, R. J. Gildea, J. A. K. Howard and H. Puschmann, *J. Appl. Crystallogr.*, 2009, **42**, 339.

17 L. N. M. E. A. Boudreux, *Theory and Applications of Molecular Paramagnetism*, John Wiley & Sons, New York, 1976.

18 Please note that the amount of base used in the two subcomponent self-assembly processes proved to be critical for the successful formation of the oligonuclear supramolecular architectures as single crystalline $Dy_6(L)_6$ and $D_{12}(L)_8$ could only be obtained using the relative ratios given in the experimental part.

19 Please note that all attempts to assemble the oligonuclear complexes from the preformed protonated ligand $H_2(L)$ were not successful.

20 (a) B. Bocquet, G. Bernardinelli, N. Ouali, S. Floquet, F. Renaud, G. Hopfgartner and C. Piguet, *Chem. Commun.*, 2002, 930; (b) K. Zeckert, J. Hamacek, J.-P. Rivera, S. Floquet, A. Pinto, M. Borkovec and C. Piguet, *J. Am. Chem. Soc.*, 2004, **126**, 11589; (c) J. Hamacek, S. Blanc, M. Elhabiri, E. Leize, A. Van Dorsselaer, C. Piguet and A.-M. Albrecht-Gary, *J. Am. Chem. Soc.*, 2003, **125**, 1541.

21 B. Wang, Z. Zang, H. Wang, W. Dou, X. Tang, W. Liu, Y. Shao, J. Ma, Y. Li and J. Zhou, *Angew. Chem., Int. Ed.*, 2013, **52**, 3756.

22 (a) J.-M. Senegas, S. Koeller, G. Bernardinelli and C. Piguet, *Chem. Commun.*, 2005, 2235; (b) S.-Y. Lin, L. Zhao, Y.-N. Guo, P. Zhang, Y. Guo and J. Tang, *Inorg. Chem.*, 2012, **51**, 10522; (c) L. Zhang, P. Zhang, L. Zhao, J. Wu, M. Guo and J. Tang, *Inorg. Chem.*, 2015, **54**, 5571.

23 T. Y. Bing, T. Kawai and J. Yuasa, *J. Am. Chem. Soc.*, 2018, **140**, 3683.

24 J. Lu, V. Montigaud, O. Cador, J. Wu, L. Zhao, X.-L. Li, M. Guo, B. Le Guennic and J. Tang, *Inorg. Chem.*, 2019, **58**, 11903.

25 (a) B. Hasenknopf, J.-M. Lehn, B. O. Kneisel, G. Baum and D. Fenske, *Angew. Chem., Int. Ed.*, 1996, **35**, 1838; (b) P. L. Jones, K. J. Byrom, J. C. Jefferey, J. A. McCleverty and M. D. Ward, *Chem. Commun.*, 1997, 1361; (c) B. Hasenknopf, J.-M. Lehn, N. Boumediene, A. Dupont-Gervais, A. Van Dorsselaer, B. Kneisel and D. Fenske, *J. Am. Chem. Soc.*, 1997, **119**, 10956; (d) B. Hasenknopf, J.-M. Lehn, N. Boumediene, E. Leize and A. Van Dorsselaer, *Angew. Chem., Int. Ed.*, 1998, **37**, 3265; (e) C. S. Campos-Fernandes, B. L. Schottel, H. T. Chifotides, J. K. Bera, J. Bacsa, J. M. Koomen, D. H. Russell and K. R. Dunbar, *J. Am. Chem. Soc.*, 2005, **127**, 12909; (f) S. P. Argent, H. Adams, T. Riis-Johannessen, J. C. Jefferey, L. P. Harding, O. Mamula and M. D. Ward, *Inorg. Chem.*, 2006, **45**, 3905; (g) H. B. Tanh Jeazet, K. Gloe, T. Doert, O. N. Kataeva, A. Jäger, G. Geipel, G. Bernhard, B. Büchner and K. Gloe, *Chem. Commun.*, 2010, **46**, 2373; (h) C. Klein, C. Gütz, M. Bogner, F. Topić, K. Rissanen and A. Lützen, *Angew. Chem., Int. Ed.*, 2014, **53**, 3739.

26 Please note that the use of amino-2-propanol instead of NEt_3 also gave rise to the same $Dy_6(L)_6$ architecture; however, its structure could not be completely satisfactorily resolved based on the single crystal XRD analysis (see the ESI†).

27 (a) M. D. Wise, J. J. Holstein, P. Pattison, C. Besnard, E. Solari, R. Scopelliti, G. Bricogne and K. Severin, *Chem. Sci.*, 2015, **6**, 1004; (b) M. Käseborn, J. J. Holstein, G. H. Clever and A. Lützen, *Angew. Chem., Int. Ed.*, 2018, **57**, 12171.

28 Some further reviews on lanthanide single-molecule magnets not covered by ref. 1: (a) D. Gatteschi, R. Sessoli and R. Villain, *Molecular Nanomagnets*, Oxford University Press, Oxford, 2006; (b) D. N. Woodruff, R. E. Winpenny and R. A. Layfield, *Chem. Rev.*, 2013, **113**, 5110; (c) H. L. C. Feltham and S. Brooker, *Coord. Chem. Rev.*, 2014, **276**, 1; (d) F. Pointillart, O. Cador, B. LeGuennic and L. Ouahab, *Coord. Chem. Rev.*, 2017, **346**, 150; (e) S. G. McAdams, A.-M. Ariciu, A. K. Kostopoulos, J. P. S. Walsh and F. Tuna, *Coord. Chem. Rev.*, 2017, **346**, 216; (f) J.-L. Liu, Y.-C. Chen and M.-L. Tong, *Chem. Soc. Rev.*, 2018, **47**, 2431; (g) F.-S. Guo, A. K. Bar and



R. A. Layfield, *Chem. Rev.*, 2019, **119**, 8479; (h) Z. Zhu, X.-L. Li, S. Liu and J. Tang, *Inorg. Chem. Front.*, 2020, **7**, 3315.

29 Y.-N. Guo, G.-F. Xu, P. Gamez, L. Zhao, S.-Y. Lin, R. Deng, J. Tang and H.-J. Zhang, *J. Am. Chem. Soc.*, 2010, **132**, 8538.

30 (a) I. J. Hewitt, J. Tang, N. T. Madhu, C. E. Anson, Y. Lan, J. Luzon, M. Etienne, R. Sessoli and A. K. Powell, *Angew. Chem., Int. Ed.*, 2010, **49**, 6352; (b) R. J. Blagg, C. A. Muryn, E. J. L. McInnes, F. Tuna and R. E. P. Winpenny, *Angew. Chem., Int. Ed.*, 2011, **50**, 6530; (c) R. J. Blagg, F. Tuna, E. J. L. McInnes and R. E. P. Winpenny, *Chem. Commun.*, 2011, **47**, 10587; (d) P.-H. Guo, J. Liu, Z.-H. Wu, H. Yan, Y.-C. Chen, J.-H. Jia and M.-L. Tong, *Inorg. Chem.*, 2015, **54**, 8087; (e) T. Pugh, V. Vieru, L. F. Chibotaru and R. A. Layfield, *Chem. Sci.*, 2016, **7**, 2128; (f) T. Pugh, N. F. Chilton and R. A. Layfield, *Chem. Sci.*, 2017, **8**, 2073; (g) J. Xiong, H.-Y. Ding, Y.-S. Meng, C. Gao, X.-J. Zhang, Z.-S. Meng, Y.-Q. Zhang, W. Shi, B.-W. Wang and S. Gao, *Chem. Sci.*, 2017, **8**, 1288; (h) J. D. Rinehart, M. Fang, W. J. Evans and J. R. Long, *J. Am. Chem. Soc.*, 2011, **133**, 14236; (i) R. J. Blagg, L. Ungur, F. Tuna, J. Speak, P. Comar, D. Collison, W. Wernsdorfer, E. J. L. McInnes, L. F. Chibotaru and R. E. P. Winpenny, *Nat. Chem.*, 2013, **5**, 673; (j) C. A. Gould, K. R. McClain, D. Reta, J. G. C. Kragskow, D. A. Marchiori, E. Lachman, E.-S. Choi, J. G. Analytis, R. D. Britt, N. F. Chilton, B. G. Harvey and J. R. Long, *Science*, 2022, **375**, 198.

